X-ray spectroscopic study of the electronic structure of $Y_{1-x}Pr_xBa_2Cu_3O_7$

H. Yamaoka,[1] H. Oohashi,[2] I. Jarrige,[3] T. Terashima,[4] Y. Zou,[5] H. Mizota,[5] S. Sakakura,[5] T. Tochio,[6] Y. Ito,[5] E. Ya. Sherman,[7] and A. Kotani[1,8]

[1]*Harima Institute, RIKEN (The Institute of Physical and Chemical Research), Sayo, Hyogo 679-5148, Japan*

[2]*Harima Office, National Institute for Materials Science, Sayo, Hyogo 679-5148, Japan*

[3]*Synchrotron Radiation Research Unit, Japan Atomic Energy Agency, 1-1-1 Kouto, Sayo, Hyogo 679-5148, Japan*

[4]*Research Center for Low Temperature and Materials Sciences, Kyoto University, Uji, Kyoto 611-0011, Japan*

[5]*Institute for Chemical Research, Kyoto University, Uji, Kyoto 611-0011, Japan*

[6]*Keihanna Interaction Plaza Incorporated, Kyoto 619-0237, Japan*

[7]*Department of Physics and Institute for Optical Sciences, University of Toronto, 60 St. George Street, Toronto, Ontario, Canada M5S 1A7*

[8]*Photon Factory, Institute of Materials Structure Science, High Energy Accelerator Research Organization, 1-1 Oho, Tsukuba, Ibaraki 305-0801, Japan*

(Received 13 September 2007; revised manuscript received 8 November 2007; published 30 January 2008)

We present a detailed investigation of the bulk electronic properties of $Y_{1-x}Pr_xBa_2Cu_3O_7$ (YPrBCO) using x-ray absorption spectroscopy in the partial fluorescence yield mode (PFY-XAS) at Pr L_3, Ba L_3, and Cu K edges together with Pr $2p_{3/2}3d_{5/2}$ and Cu $1s2p$ resonant inelastic x-ray scatterings. Pr L_3 PFY-XAS spectra show that Pr is in the mixed-valence state (with the valence number slightly greater than 3) for the whole $x=0.2-1$ range, while the Pr valence decreases with increasing x. The decrease of the Pr^{4+} component upon Pr doping, hinting at a weakening Pr-O hybridization, is inconsistent with the scenario according to which the increase in Pr-O hybridization quenches the superconductivity in YPrBCO for $x \geqslant 0.6$. It rather suggests that the superconductivity may be suppressed by the total increase of the Pr-related states in the electronic structure due to the Pr ion concentration upon doping. No doping dependence is found in the electronic structure of the Ba and Cu sites, consistent with their invariant environment. No temperature dependence in our data is observed within the experimental accuracy.

DOI: 10.1103/PhysRevB.77.045135 PACS number(s): 75.30.Mb, 61.05.cj, 71.20.Eh, 78.70.Ck

I. INTRODUCTION

Most $RBa_2Cu_3O_y$ (RBCO, R: rare earth, $y \simeq 7$) compounds exhibit high superconducting transition temperature (T_c) of about 90 K.[1–5] T_c decreases[6] when increasing the ion radius. The compounds with R=Pr (PrBCO) and Pr substitution of Y at the R site [$Y_{1-x}Pr_xBa_2Cu_3O_7$ (YPrBCO), $x \geqslant 0.6$] are unique in the series for their completely suppressed superconductivity. Understanding this anomalous behavior is expected to shed light on the underlying mechanism of superconductivity in high T_c cuprates. Although an abundance of studies have been performed for the past 20 years in connection with the quenched superconductivity in the Pr-doped systems, the experimental results are sometimes inconsistent and the exact mechanism has not been concluded yet.[5]

A number of models have been proposed for the origin of the anomalous properties of PrBCO and YPrBCO, such as hole filling,[7] hole localization,[8] percolation,[9] magnetic pairbreaking,[7,10,11] magnetic impurity scattering,[12] Pr-O hybridization [Fehrenbacher-Rice (FR) theory],[13,14] disorder of Ba site,[15] hole transfer from CuO_2 planes to CuO chains,[16] and mis-substitution effect of Pr atom in Ba site.[17,18] The most commonly accepted one appears to be the Pr-O hybridization, according to which hybridization between Pr $4f$ and O $2p$ binds holes primarily from the CuO_2 planes to tetravalent Pr sites, which in turn destroys the superconductivity.[13,14] There is, however, no unified theory that can describe all experimental results, including the nonlinear change in T_c with the Pr concentration. For example, theoretical analysis of Yu *et al.*[19] suggested the presence of three regimes in the $T_c(x)$ dependence, with a decrease in T_c associated with the transition from overdoping to underdoping at small x, effects of hole depletion and pair breaking dominating the middle x region, and mostly pair breaking remaining at $x > 0.5$. On the other hand, Tomkowicz[20] suggested that the $T_c(x)$ dependence can be explained solely by trapping of the holes at Pr ion sites. Another anomaly in PrBCO is the high magnetic ordering temperature of 17 K,[4] similar to CmBCO.[12]

Unveiling the electronic structure, including the valence state, of YPrBCO is a mandatory ingredient to understand its unusual behavior. X-ray spectroscopy is a powerful tool to derive such information. In previous works, particular attention has been paid to the Pr valence for its variation as a function of the Pr concentration x. Thus, the ratio of the Pr^{4+} component was reported to be inversely proportional to x by means of x-ray absorption spectroscopy (XAS).[21–24] Neukirch *et al.* suggested an upper limit of 10% on the relative Pr^{4+} content in YPrBCO by means of Pr M and Pr L edge XASs.[25] Yet, Hilscher *et al.*[26] found an admixture of ~15% of Pr^{4+} using XAS at the Pr L_3 and Pr L_2 edges.

Besides, drastic changes were found in the intensity of the O K edge XAS spectrum as a function of x.[27–31] These changes have been understood on the basis of a decrease (increase) of the Zhang-Rice [Fehrenbacher-Rice (FR)] state with increasing Pr concentration, the Zhang-Rice (ZR) states being related to the hole states in the superconducting CuO_2 planes. Thus, the hole transfer from the ZR states to the localized FR states, occurring through the hybridization be-

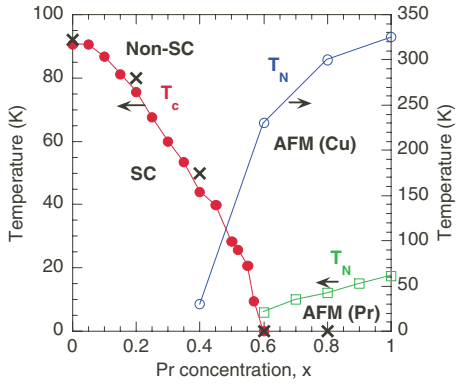

FIG. 1. (Color online) Superconducting transition temperature (T_c) and Néel temperature (T_N) as a function of Pr concentration (x) for $Y_{1-x}Pr_xBa_2Cu_3O_7$. The closed circle, cross, open circle and open square are the data from Tomkowicz (Ref. 20), this study, Felner *et al.* (Ref. 34), and Kobede *et al.* (Ref. 35), respectively.

tween the O $2p\pi$ and Pr $4f_{z(x^2-y^2)}$ orbitals, was suggested to result in a significant decrease of the hole number in the CuO_2 planes with increasing x.

In this paper, we report on a comprehensive spectroscopic study of the bulk electronic properties of $Y_{1-x}Pr_xBa_2Cu_3O_7$ (x=0, 0.2, 0.4, 0.6, and 0.8) using recently developed techniques, x-ray absorption spectroscopy in the partial fluorescence yield (PFY-XAS) and resonant inelastic x-ray scattering (RIXS). Owing to the site selectivity of the PFY-XAS measurement, we could obtain high-resolution Pr L absorption spectra free of the Ba L_1 absorption signal which usually overlaps with the high-energy part of the Pr L edge. This allows us to accurately derive the x dependence of the Pr valence and show that the Pr^{4+} component decreases with increasing doping, especially in the 0.2–0.4 range. The RIXS spectra were previously shown to provide detailed and reliable information about the electronic structure of f electron systems, such as the degree of localization and electronic occupancy.[32,33] The Pr $2p_{3/2}3d_{5/2}$ RIXS spectra are suggestive of delocalized, partially hybridized Pr $5d$ states. No Pr-doping dependence was found in the Ba and Cu absorption edges, consistent with their invariant structural environment. Besides, no temperature dependence was observed in our data.

II. EXPERIMENTS

A. Sample

Samples of $Y_{1-x}Pr_xBa_2Cu_3O_7$ (x=0, 0.2, 0.4, 0.6, and 0.8) are prepared from a mixture of pure oxides by the standard solid state reaction method. Magnetic susceptibility measurements on our samples as a function of temperature showed the superconducting transition at temperature T_c. Our dependence of T_c on Pr concentration (cross points) is reported in Fig. 1 along with the data from Ref. 20 and the Néel temperature (T_N) from Refs. 34 and 35. Our results are consistent with those of Ref. 20. The superconducting character is observed to disappear for $x \geqslant 0.6$.

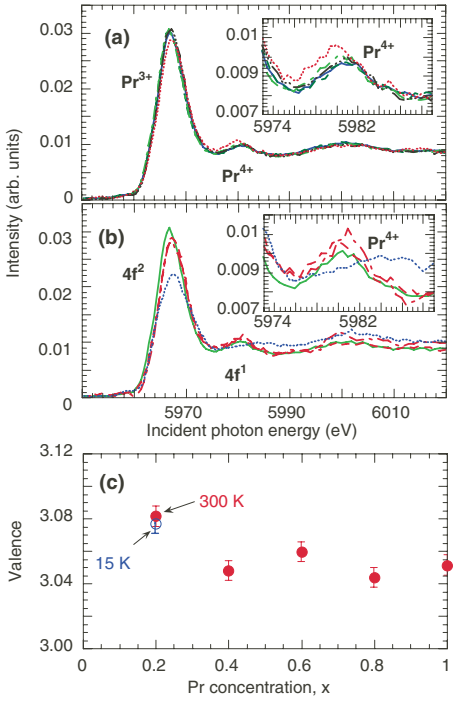

FIG. 2. (Color online) Pr L_3 PFY-XAS spectra obtained for $Y_{1-x}Pr_xBa_2Cu_3O_7$ (a) x dependence at 300 K; x=0.2 (dotted line, red), 0.4 (long-dashed-triple-dotted line, black), 0.6 (long-dashed-dotted line, light green), 0.8 (broken line, green), and 1.0 (solid line, blue). (b) Temperature dependence; x=0.2 at 15 K (long-dashed-dotted line, red), 0.2 at 300 K (broken line, red), and 0.6 at 300 K (solid line, green) along with the Pr_2O_3 spectrum (dotted line, blue). (c) Estimated mean valence from PFY-XAS spectra as a function of Pr concentration (x). Inserted figures are enlarged $4f^1$ regions.

B. Measurement

X-ray spectroscopic measurements are performed at the undulator beamline BL15XU (Ref. 36) in SPring-8. The undulator beam is monochromatized by a water-cooled double crystal monochromator. Energy calibration of the beamline monochromator is performed at the Cu K edge. The incident beam intensity is monitored by a thin Al foil located just before the sample. X-ray emission is measured by Ge 111 double crystal spectrometer with (+,+) geometry.[37] Ge 111 lattice constant has been estimated before[38] and energy calibration of the spectrometer is performed between Pr $L\alpha_1$ and Cu $K\alpha_1$ emission lines. The resolution $E/\delta E$ is estimated to be about 3350 at 8050 eV, where E is the photon emission energy. We used an Iwatani CRT-M310-OP cryostat to cool down the samples from room temperature to about 15 K.

III. RESULTS AND DISCUSSION

A. X-ray absorption spectroscopy in the partial fluorescence yield mode

Figure 2 shows the Pr L_3 PFY-XAS spectra obtained for $Y_{1-x}Pr_xBa_2Cu_3O_7$ as a function of x and temperature together with the Pr_2O_3 reference spectrum [Fig. 2(b)]. All the spectra are normalized to their area. They were measured by tuning

the spectrometer energy to the peak of the Pr $L\alpha_1$ emission line while scanning the incident photon energy across the Pr L_3 edge. The PFY-XAS technique yields spectra with sharper features than conventional absorption, offering a higher accuracy when deriving quantitative information such as the valence. Moreover, in the present case, we measure the intensity variation of a Pr emission line; our spectra are therefore free from the Ba L_1 edge signal which would appear above 5989 eV in a conventional absorption spectrum. We note that, although measuring at the Pr L_2 absorption edge would allow us to circumvent the Ba signal as well, Lytle *et al.* reported the absence of Pr 4+ peak at the L_2 XAS spectrum for $x=0.6$.[21]

We ascribe the two peaks at 5968 and 5980 eV in the spectra of YPrBCO to the main edge ($2p \rightarrow 5d$ transition) of the Pr^{3+} ($4f^2$) and Pr^{4+} ($4f^1$) sites, respectively.[39] The intensity of the $4f^1$ peak decreases for YPrBCO between $x=0.2$ and 0.4, while, as expected, the Pr_2O_3 spectrum seems to have no $4f^1$ contribution.

We estimate the Pr valence v with the formula $v=3+I(4f^1)/[I(4f^2)+I(4f^1)]$, where $I(4f^n)$ is the intensity of the $4f^n$ component. In order to estimate $I(4f^n)$, we subtract from the PFY-XAS spectra the arctanlike transitions into the continuum and fit the remaining spectral density with Voigt functions. The results, plotted in Fig. 2(c), interestingly show that $Y_{1-x}Pr_xBa_2Cu_3O_7$ always remains in the mixed-valence state, the valence decreasing between $x=0.2$ and 0.4 and then showing little variations over the $x=0.4-1.0$ range.

Our value of the valence at $x=0.2$, 3.08 ± 0.01, is smaller than the XAS derived values of 3.4 ± 0.2 for $x=0.2$ and 3.18 ± 0.05 for $x=1$ of Alleno *et al.*[23] and 3.45 for $x=0.2$ and 3.25 for $x=0.6$ of Lytle *et al.*[21] It is, however, in good agreement with those of Staub *et al.*[40,41] and Ku *et al.*[39] estimated using XAS, too. At small Pr concentrations, the contribution from the Ba L_1 edge in the Pr L_3 spectrum becomes relatively larger and, because it is located only a few eV above the weak Pr^{4+} component in the normal XAS spectrum, may affect the estimation of the Pr valence. Our site-selective and high-resolution absorption spectra are therefore expected to yield a more reliable value of the Pr valence. Besides, our results are qualitatively consistent with most of the previous XAS works on that increasing the Pr concentration results in decreasing its valence. This phenomenon was accounted for by the calculations of Tanaka and Motoi[42] using the ionic crystal model.

Here, it is noted that Staub *et al.*[40] and Ku *et al.*[30] showed that the Pr valence increases with oxygen concentration. Thus, Staub *et al.* reported a change in the valence from 3.09 for $\delta=0$ to 3.05 for $\delta=1$ in $Y_{1-x}Pr_xBa_2Cu_3O_{7-\delta}$. Although we did not measure the oxygen content in our samples, we can reasonably assume that the change in δ from one sample to another is much less than 1. Accordingly, the valence difference we derived between $x=0.2$ and 0.4, ~0.03, should be very poorly affected by the possible difference in oxygen content.

The mean Pr-O distance in YPrBCO has been previously reported to increase as a function of x by means of x-ray diffraction[44] and extended x-ray absorption fine structure (EXAFS).[24] In the latter study, the valence of Pr was estimated to be 4+ for $x=0$ and 3+ for $x=1$. Our results somewhat support this trend qualitatively.

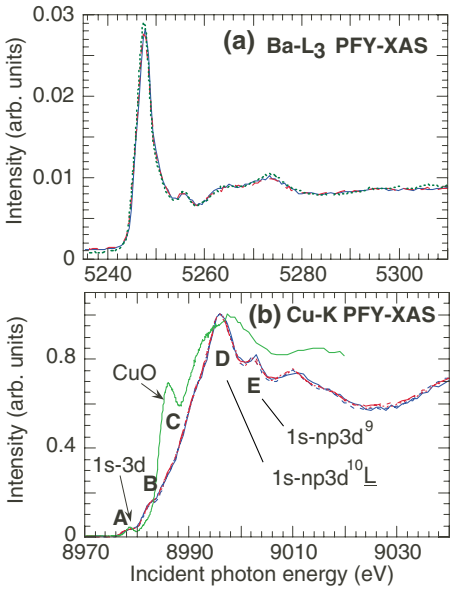

FIG. 3. (Color online) PFY-XAS spectra obtained for $Y_{1-x}Pr_xBa_2Cu_3O_7$ at the (a) Ba L_3 with $x=0.2$, 15 K (dotted line, green), $x=0.2$, 300 K (dashed-dotted line, red), and $x=0.6$, 300 K (solid line, blue) and (b) Cu K edges for $x=0.2$ at 15 K (dotted line, red) and 300 K (dashed-double-dotted line, red) and 0.6 at 15 K (broken line, blue) and 300 K (solid line, blue). In (b), the CuO PFY spectrum at 300 K (solid line, green) is also shown.

The Pr^{4+} state was found to split over two peaks in the L_3 absorption spectrum of PrO_2, $4f^1$ and $4f^2\underline{L}$ states, where $\underline{L}$ is a hole in O $2p$ orbital.[43] These two peaks are separated by ~9.4 eV. Through the curve fit assuming the energy separation of 9.4 eV also for YPrBCO, we derive the intensity of the $4f^2\underline{L}$ component, which overlaps with the tail of the strong $4f^2$ state of Pr^{3+} in Fig. 2. Accounting for these two distinct Pr^{4+} peaks in the fit, the valence is estimated to be about 3.25 ± 0.05 at $x=0.2$ from the formula $v=3+[I(4f^1)+I(4f^2\underline{L})]/[I(4f^2)+I(4f^1)+I(4f^2\underline{L})]$. Nevertheless, the x dependence of the valence remains qualitatively the same.

Figure 3(a) shows Ba L_3 PFY-XAS spectra, collected by monitoring the intensity variations of the $L\alpha_1$ ($2p_{3/2}-3d_{5/2}$) emission line for the $x=0.2$ (15 and 300 K) and 0.6 (300 K) samples. No x dependence is observed, which suggests that the Ba sites are not affected by Pr substitution. A similar observation was made from the Ba $5p \rightarrow$ Ba $4d$ soft x-ray emission spectrum.[45] This result is consistent with the EXAFS measurements of Gurman *et al.*,[24] which reported no change for the environment of the Ba sites over Pr doping.

Figure 3(b) shows the Cu K PFY-XAS spectra obtained by measuring the incident energy variations of the Cu $K\alpha_1$ emission line for the $x=0.2$ and 0.6 samples at 15 and 300 K, along with the CuO spectrum. The resemblance with the CuO spectrum shows that Cu is near the 2+ charge state. No change seems to occur in the spectra as a function of x or temperature. Tanaka and Motoi studied the Cu electronic state in YPrBCO using the valency model[42] and suggested that, since the Pr valence is higher than that of Y by about 0.3, a slight reduction of the Cu valence in the CuO_2 planes is likely to occur upon Pr doping. They predicted a decrease

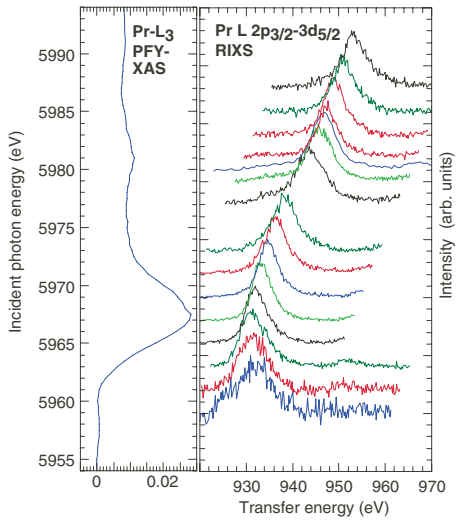

FIG. 4. (Color online) Pr $2p_{3/2}3d_{5/2}$ RIXS spectra for YPrBCO $x=0.2$ at 15 K as a function of the incident photon energies (right panel) along with the Pr L_3 edge (left panel). The vertical scale of the right panel corresponds to x-ray intensity. The position of the base line of each spectrum in the right panel scales to the energy of the left panel.

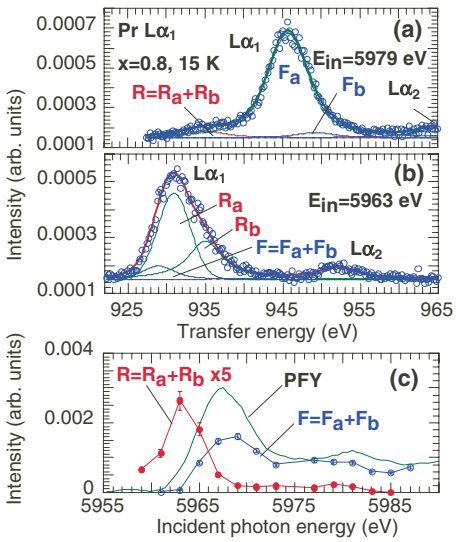

FIG. 5. (Color online) Examples of the curve fit of the Pr $2p_{3/2}3d_{5/2}$ RIXS spectra obtained for YPrBCO ($x=0.2$) at 15 K and incident photon energies of E_{in}= (a) 5979 eV and (b) 5963 eV. The open circles are the experimental spectra. R_a and R_b are Raman components and F_a and F_b are fluorescence components. (c) Incident photon energy dependence of the intensity of the fluorescence (open circle, $F=F_a+F_b$) and Raman components (closed circle, $R=R_a+R_b$) with PFY (solid line). The intensity of the Raman component is multiplied by a factor of 5.

of about 0.05 in the valence of the Cu(2) site, while the valence of the Cu(1) site remains unchanged as the Pr concentration is changed between $x=0$ and 1. Our measurement yields information averaged over the two Cu sites, so one can think that the weak changes remain within the error bar. On the other hand, the environment of the Cu atoms was found invariant over Pr doping by EXAFS, which is suggestive of a constant Cu valence.[24]

B. Resonant inelastic x-ray scattering for Pr

We collected the Pr $2p_{3/2}3d_{5/2}$ RIXS spectra for the $x=0.2$ sample at 15 K, where superconductivity is observed. Figure 4 shows the corresponding RIXS spectra along with the Pr L_3 PFY-XAS spectrum. The RIXS spectra are normalized to their peak intensity and plotted as a function of the transfer energy, defined as the difference between the incident and emitted photon energies. Going from low to high incident photon energy, one can successively observe the Raman regime where the signal remains at constant transfer energy and the fluorescence regime where the peak drifts toward the high transfer energy side.[46] At 5978 eV, the $L\alpha_1$ emission line is observed to broaden, which we suppose is due to the overlap of the Pr $4f^1$ and Pr $4f^2$ components. In order to separate the Raman and fluorescence components, we fit the whole series of spectra, as illustrated in Fig. 5.[38] For the fluorescence signals, we need to assume a sum of two symmetrical lines, main F_a and small F_b, so as to account for the multiplet effects under the existence of the core hole.[47] For the Raman regime, too, two components, R_a and R_b, are necessary. The results of the curve fit are summarized in Fig. 5(c), where $F=F_a+F_b$ and $R=R_a+R_b$.

Our Pr $2p_{3/2}3d_{5/2}$ RIXS spectra resemble the Gd $2p_{3/2}3d_{5/2}$ ones obtained for $Gd_3Ga_5O_{12}$.[48] In the $Gd_3Ga_5O_{12}$ case, the Raman component due to the quadrupolar transition was detected. A similar weak feature of quadrupolar origin can be seen in our PFY-XAS spectrum, too, at the incident energy of 5959 eV. The dipole transition associated with the Raman component in $Gd_3Ga_5O_{12}$ was found to be stronger than the fluorescence signal for incident energies as high as the maximum of the main absorption edge. Rueff *et al.* suggested that it is possible to characterize the degree of covalence or localization of the states near the Fermi level based on the incident energy dependence of the so-called Raman and fluorescent features in the preedge region.[49] The transitions to the localized intermediate states belong to the Raman regime and are expected to appear at constant transfer energy. The transfer energy of the transitions to the band states disperses linearly with the incident energy. The degree of delocalization of the electronic states depends on the incident energy range over which the transitions to these respective states take place. For example, if the Raman regime is extended up to the absorption edge, the states are said to be relatively localized, whereas Raman transitions confined to the preedge would point to a relative delocalization. In comparison, the Raman component in our case is restricted to a few eV below the edge, so we can conclude to a relative delocalization (or hybridization) of the Pr $5d$ states in YPrBCO because the Raman component of Pr corresponds to the $2p$-$5d$ transition.

C. Resonant inelastic x-ray scattering for Cu

The Cu $1s2p$ RIXS spectra measured for the $x=0.2$ and 0.6 samples at 15 K are displayed in Fig. 6, where Figs. 6(b)

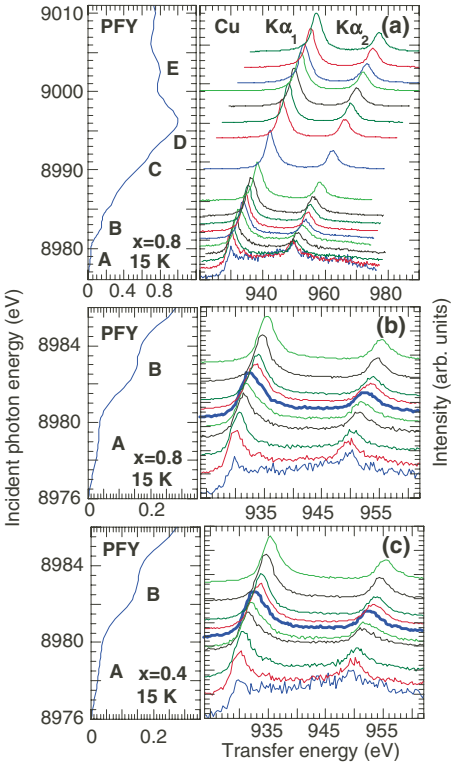

FIG. 6. (Color online) (a) Cu $1s2p$ RIXS spectra obtained for YPrBCO at $x=0.2$, 15 K as a function of the incident photon energies along with the Cu K PFY-XAS edge. (b) Enlarged preedge region of (a). (c) Enlarged preedge region for $x=0.6$ at 15 K. The position of the base line of each spectrum in the right panel scales to the energy of the left panel.

and 6(c) show the enlarged preedge region. The $x=0.2$ and 0.6 spectra strongly resemble each other. The Raman regimes are restricted mainly to the pre-edge peak region. We observe a broadening of the spectral features for an incident energy of 8980 eV. A similar phenomenon was observed in La_2CuO_4,[50] accounted for by coexisting on-site (quadrupole) and off-site (dipole) Cu $1s$-Cu $3d$ transitions by means of many body cluster calculations.

The Cu $K\alpha$ emission spectra for CuO, YPrBCO, and Cu metal obtained for incident energies $E_{in}=9005-9020$ and the corresponding Cu $1s2p$ RIXS spectra measured at $E_{in}=8976$ eV are plotted in Fig. 7. The three fluorescence spectra are found to be similar with each other. The CuO $1s2p$ RIXS spectrum shows three distinguishable peaks, referred to as C, A, and S in Ref. 51. The same peaks, even though less clear, are still observed in the YPrBCO spectra. Peak C was proposed to originate from the $1s^{-1}3d^{10}$ intermediate state ($1s$-$3d$ transition).[51] These three peaks show a constant transfer energy with E_{in}; therefore, they are Raman components.

Examples of the curve fit of the Cu $1s2p$ RIXS spectra are shown in Fig. 8 for $E_{in}=8982$, 8977 eV. For the Cu $K\alpha$ fluorescence, based on the results of Deutsch *et al.*, we assumed two lines, $K\alpha_{11}$ (main peak) and $K\alpha_{12}$ (weak satellite peak) for $K\alpha_1$.[52] For the Raman components, three peaks ($R1-R3$) were necessary in the preedge peak region, as shown in Fig.

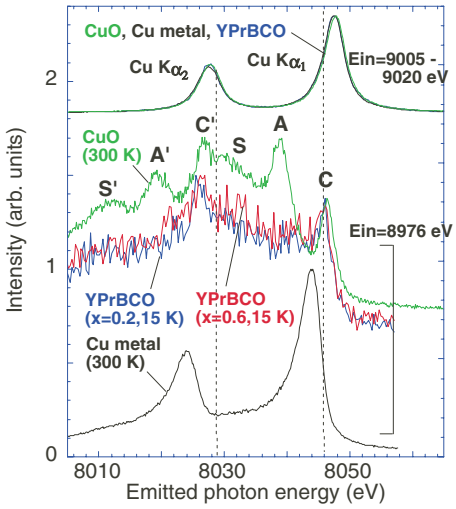

FIG. 7. (Color online) Cu $K\alpha$ emission spectra obtained for CuO, YPrBCO, and Cu metal at the incident energies of $E_{in}=9005-9020$ and Cu $1s2p$ RIXS spectra obtained for 8976 eV. The notations (C, A, S) for the RIXS spectra follow Ref. 51.

8(b). $R1$ and $R3$ seem to correspond, respectively, to C ($1s$-$3d$) and A in Fig. 7 (see in Ref. 51). $R3$ seems to be associated with broadening of the RIXS spectrum obtained for an incident photon energy of 8980 eV (cf. Fig. 6).

Figure 9 shows the results of the curve fit. Whereas the fluorescence signals extend to the whole edge, the quadrupolar Raman components $R1$ and $R3$ are observed only in the preedge region. The Raman component $R2$ corresponds to the dipolar transition ($1s$-$4p$) and is mainly restricted below the main absorption peak D. These results suggest relative delocalization of the Cu $3d$ and Cu $4p$ states.

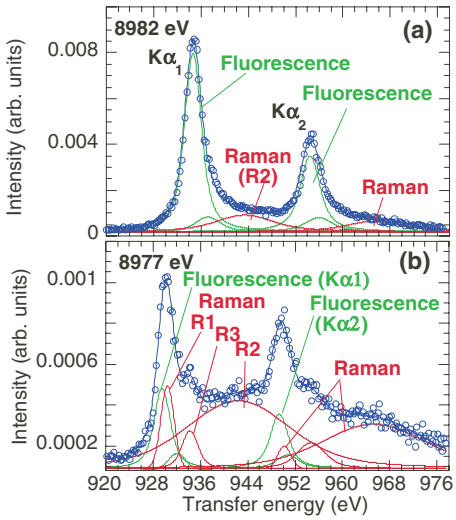

FIG. 8. (Color online) Example of curve fit shown for the Cu $1s2p$ RIXS spectra obtained for YPrBCO ($x=0.2$) at 15 K and incident photon energies of (a) 8982 eV and (b) 8977 eV. The open circles are the experimental data.

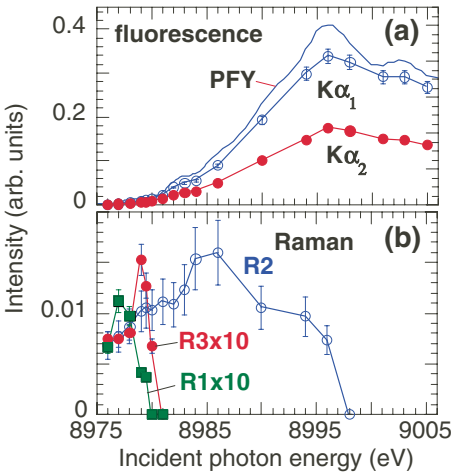

FIG. 9. (Color online) Incident photon energy dependence of the intensity of (a) the fluorescence components Cu $K\alpha_1$ and Cu $K\alpha_2$ and (b) the Raman components $R1$, $R2$, $R3$ of the Cu $1s2p$ RIXS spectra obtained for YPrBCO ($x=0.2$) at 15 K.

D. Effect of the Pr doping on the electronic states

The Pr^{3+} ion radius is about 11% larger than that of Y^{3+} (Ref. 5). Increasing the substitution degree of the Y sites by Pr is therefore expected to result in an increased lattice parameter and Pr-O interatomic distance, as was previously observed by EXAFS.[24] Then, as the Pr-O distance increases, the hole transfer from O to Pr becomes less likely, thus causing the Pr valence to decrease as we observed by PFY-XAS at the Pr L_3 edge. Our results of the Pr valence are therefore consistent with the increase of the Pr-O distance upon Pr doping.

One can think of another interpretation of the Pr valence decrease based on the picture that, when the Pr ions are far away from each other (low Pr content), each Pr ion strongly interacts with the holes and attracts them to it. When the Pr concentration is increased, the minima of the effective potential become more spread and there is no need for the holes to be located too closely to the Pr ions, thus leading to the observed valence decrease.

On the other hand, measurements of the O $1s$ absorption spectra suggested that hole carriers in the CuO_2 planes and CuO chains decrease with Pr doping, which was ascribed to the hole transfer from the ZR band to the FR states occurring via the Pr $4f$-O $2p$ hybridization and which would result in an enhanced stabilization of the Pr^{4+} state.[27–31] Although our observation of the mixed valence of Pr at all doping levels supports the idea that Pr doping always induces hole transfer from O to Pr site through Pr-O hybridization, we show here that this hybridization decreases over Pr doping. This invalidates the scenario according to which the increase in the Pr-O hybridization at the unit cell scale suppresses the superconductivity.[27–31] Instead, we suggest that with the increase in Pr content, as a whole, the presence of Pr-related electron states and corresponding modifications of the total electron structure may affect the superconductivity.

IV. CONCLUSION

Site-selective Pr K PFY-XAS measurements indicate that the Pr valence is slightly larger than 3 and decreases with Pr doping, especially over the 0.2–0.4 range. This result is understood in terms of weakening of the Pr-O hybridization caused by the increase of the Pr-O distance upon doping. No change is observed in the electronic structure of Ba and Cu upon doping, which is consistent with their invariant environment. Cu K PFY-XAS spectra show that the Cu mean valence is nearly 2+. RIXS spectra obtained at the Pr L_3 edge suggest relatively delocalized $5d$ states. Our results show that the suppression of the superconductivity for $x \geqslant 0.6$ is unlikely to stem from the increase in Pr-O hybridization. Instead, one of the different possible mechanisms suggested here is the increase in the Pr-related states due to the Pr ion concentration upon doping which, as a whole, strongly modifies the electron states in a way that the transition temperature is reduced or suppressed. No temperature dependence was observed for our data within the experimental accuracy.

ACKNOWLEDGMENTS

The experiments were performed at BL15XU (Proposal No. 2006A1607) of SPring-8, Japan Synchrotron Radiation Research Institute (JASRI). We thank H. Yoshikawa, Y. Katsuya, and D. Nomoto in BL15XU for the experimental help. We also deeply appreciate M. Taguchi and A. Chainani in RIKEN for the fruitful discussion.

[1] K. N. Yang, Y. D. Dalichaouch, J. M. Ferreira, R. R. Hake, B. W. Lee, J. J. Neumeier, M. S. Torikachvili, H. Zhou, and M. B. Maple, Jpn. J. Appl. Phys., Suppl. **26**, 1037 (1987).
[2] H. B. Radousky, J. Mater. Res. **7**, 1917 (1992).
[3] I. I. Mazin, AIP Conf. Proc. **483**, 77 (1999).
[4] A. T. Boothroyd, J. Alloys Compd. **303-304**, 489 (2000).
[5] M. Akhavan, Physica B **321**, 265 (2002).
[6] Y. Xu and W. Guan, Phys. Rev. B **45**, 3176 (1992); J. C. Chen, Y. Xu, M. K. Wu, and W. Guan, *ibid.* **53**, 5839 (1996).
[7] J. J. Neumeier, T. Bjørnholm, M. B. Maple, and I. K. Schuller, Phys. Rev. Lett. **63**, 2516 (1989).
[8] J. Fink, N. Nücker, H. Romberg, M. Alexander, M. B. Maple, J. J. Neumeier, and J. W. Allen, Phys. Rev. B **42**, 4823 (1990).
[9] C. Infante, M. K. El Mously, R. Dayal, M. Husain, S. A. Siddiqi, and P. Ganguly, Physica C **167**, 640 (1990).
[10] A. Abrikosov and L. P. Gor'kov, Zh. Eksp. Teor. Fiz. **39**, 1781 (1960) [Sov. Phys. JETP **12**, 1243 (1961)].
[11] J. L. Peng, P. Klavins, R. N. Shelton, H. B. Radousky, P. A. Hahn, and L. Bernardez, Phys. Rev. B **40**, 4517 (1989).
[12] L. Soderholm and C.-K. Loong, J. Alloys Compd. **193**, 125 (1993).
[13] R. Fehrenbacher and T. M. Rice, Phys. Rev. Lett. **70**, 3471 (1993).
[14] A. I. Liechtenstein and I. I. Mazin, Phys. Rev. Lett. **74**, 1000

(1995).
[15] Y. Wang, Han Rushan, and Z.-B. Su, Phys. Rev. B **50**, 10350 (1994).
[16] D. Khomskii, J. Supercond. **6**, 69 (1993).
[17] H. A. Blackstead, D. B. Chrisey, J. D. Dow, J. S. Horwitz, A. E. Klunzinger, and D. B. Pulling, Phys. Lett. A **207**, 109 (1995).
[18] J. M. Chen, R. S. Liu, P. Nachimuthu, M. J. Kramer, K. W. Dennis, and R. W. McCallum, Phys. Rev. B **59**, 3855 (1999).
[19] Y. Yu, G. Cao, and Z. Jiao, Phys. Rev. B **59**, 3845 (1999).
[20] Z. Tomkowicz, Physica C **320**, 173 (1999).
[21] F. W. Lytle, G. van der Laan, R. B. Greegor, E. M. Larson, C. E. Violet, and Joe Wong, Phys. Rev. B **41**, 8955 (1990).
[22] M. Khaled, N. L. Saini, K. B. Garg, and F. Studer, Solid State Commun. **100**, 773 (1996).
[23] E. Alleno, C. Godart, B. Fisher, J. Genossar, L. Patlagan, and G. M. Reisner, Physica B **259-261**, 530 (1999).
[24] S. J. Gurman, J. C. Amiss, M. Khaled, N. L. Saini, and K. B. Garg, J. Phys.: Condens. Matter **11**, 1847 (1999).
[25] U. Neukirch, C. T. Simmons, P. Sladeczek, C. Laubschat, O. Strebel, G. Kaindl, and D. D. Sarma, Europhys. Lett. **5**, 567 (1988).
[26] G. Hilscher, T. Holubar, G. Schaudy, J. Dumschat, M. Strecher, G. Wortmann, X. Z. Wang, B. Hellebrand, and D. Bäuerle, Physica C **224**, 330 (1994).
[27] D. D. Sharma, P. Sen, R. Ciming, C. Carbope, W. Gudat, E. V. Sampathkumaran, and I. Das, Solid State Commun. **77**, 377 (1991).
[28] M. Merz, N. Nücker, E. Pellegrin, P. Schweiss, S. Schuppler, M. Kielwein, M. Knupfer, M. S. Golden, J. Fink, C. T. Chen, V. Chakarian, Y. U. Idzerda, and A. Erb, Phys. Rev. B **55**, 9160 (1997).
[29] J. M. Chen, R. S. Liu, J. G. Lin, C. Y. Huang, and J. C. Ho, Phys. Rev. B **55**, 14586 (1997).
[30] J. M. Chen, S. J. Liu, J. M. Lee, I. P. Hong, J.-Y. Lin, Y. S. Gou, and H. D. Yang, Chem. Phys. Lett. **370**, 180 (2003).
[31] J. M. Chen, S. J. Liu, C. F. Chang, J.-Y. Lin, Y. S. Gou, and H. D. Yang, Phys. Rev. B **67**, 014502 (2003).
[32] C. Dallera, E. Annese, J.-P. Rueff, A. Palenzona, G. Vankó, L. Braicovich, A. Shukla, and M. Grioni, Phys. Rev. B **68**, 245114 (2003).
[33] J.-P. Rueff, C. F. Hague, J.-M. Mariot, L. Journel, R. Delaunay, J.-P. Kappler, G. Schmerber, A. Derory, N. Jaouen, and G. Krill, Phys. Rev. Lett. **93**, 067402 (2004).
[34] I. Felner, U. Yaron, I. Nowik, E. R. Bauminger, Y. Wolfus, E. R. Yacoby, G. Hilscher, and N. Pillmayr, Phys. Rev. B **40**, 6739 (1989).
[35] A. Kebede, C. S. Jee, J. Schwegler, J. E. Crow, T. Mihalisin, G. H. Myer, R. E. Salomon, P. Schlottmann, M. V. Kuric, S. H. Bloom, and R. P. Guertin, Phys. Rev. B **40**, 4453 (1989).
[36] A. Nisawa, M. Okui, N. Yagi, T. Mizutani, H. Yoshikawa, and S. Fukushima, Mikrochim. Acta **497**, 563 (2003).
[37] D. Horiguchi, K. Yokoi, H. Mizota, S. Sakakura, H. Oohashi, Y. Ito, T. Tochio, A. M. Vlaicu, H. Yoshikawa, S. Fukushima, H. Yamaoka, and T. Shoji, Radiat. Phys. Chem. **75**, 1830 (2006).
[38] H. Yamaoka, M. Taguchi, A. M. Vlaicu, H. Oohashi, Y. Yokoi, D. Horiguchi, T. Tochio, Y. Ito, K. Kawatsura, K. Yamamoto, A. Chainani, S. Shin, M. Shiga, and H. Wada, J. Phys. Soc. Jpn. **75**, 034702 (2006).
[39] H. C. Ku, B. N. Lin, Y. X. Lin, and Y. Y. Hsu, J. Appl. Phys. **91**, 7128 (2002).
[40] U. Staub, L. Soderholm, S. R. Wasserman, A. G. O. Conner, M. J. Kramer, B. D. Patterson, M. Shi, and M. Knapp, Phys. Rev. B **61**, 1548 (2000).
[41] U. Staub, M. Shi, A. G. O'Conner, M. J. Kramer, and M. Knapp, Phys. Rev. B **63**, 134522 (2001).
[42] S. Tanaka and Y. Motoi, Phys. Rev. B **52**, 85 (1995).
[43] A. Bianconi, A. Kotani, K. Okada, R. Giorgi, A. Gargano, A. Marcelli, and T. Miyahara, Phys. Rev. B **38**, 3433 (1988).
[44] S. Lei, H. Yunsong, J. Yunbo, L. Xianming, Z. Guien, and Z. Yuheng, J. Phys.: Condens. Matter **10**, 7015 (1998).
[45] D. R. Mueller, J. S. Wallace, J. J. Jia, W. L. O'Brien, Q.-Y. Dong, T. A. Callcott, K. E. Miyano, and D. L. Ederer, Phys. Rev. B **52**, 9702 (1995).
[46] T. Åberg and B. Crasemann, in *Resonant Anomalous X-ray Scattering Theory and Application*, edited by G. Materlik, C. J. Sparks, and K. Fischer (Elsevier Science, New York, 1994), p. 431.
[47] A. Kotani and H. Ogasawara, J. Electron Spectrosc. Relat. Phenom. **60**, 257 (1992).
[48] M. H. Krisch, C. C. Kao, F. Sette, W. A. Caliebe, K. Hämäläinen, and J. B. Hastings, Phys. Rev. Lett. **74**, 4931 (1995).
[49] J.-P. Rueff, L. Journel, P.-E. Petit, and F. Farges, Phys. Rev. B **69**, 235107 (2004).
[50] A. Shukla, M. Calandra, M. Taguchi, A. Kotani, G. Vankó, and S.-W. Cheong, Phys. Rev. Lett. **96**, 077006 (2006).
[51] H. Hayashi, Y. Udagawa, W. A. Caliebe, and C.-C. Kao, Phys. Rev. B **66**, 033105 (2002).
[52] M. Deutsch, G. Hölzer, J. Härtwig, J. Wolf, M. Fritsch, and E. Förster, Phys. Rev. A **51**, 283 (1995).